

Hyperon-rich Matter

Jürgen Schaffner
The Niels Bohr Institute
Blegdamsvej 17
DK-2100 Copenhagen

February 9, 2008

Abstract

The phase diagram of nuclear matter offers fascinating features for heavy ion physics and astrophysics when extended to strangeness and antimatter. We will discuss some regions of this phase diagram as strange matter at zero temperature, hypermatter at high densities and the antiworld at high densities and strangeness fraction.

1 Strange Matter and Hypermatter

Relativistic heavy ion collisions provide a promising tool for studying the physics of strange quark and strange hadronic matter (see recent review [1]). Fig. 1 shows schematically the phase diagram of hot, dense and strange matter.

Perhaps the only unambiguous way to detect the transient existence of a quark gluon plasma (QGP) might be the experimental observation of exotic remnants, like the formation of strange quark matter (SQM) droplets. First studies in the context of the MIT-bag model predicted that sufficiently heavy strangelets might be metastable or even absolutely stable. The reason for the possible stability of SQM is related to a third flavour degree of freedom, the strangeness. As the mass of the strange quark is smaller than the Fermi energy of the quarks, the total energy of the system is lowered by adding strange quarks. According to this picture, the number of strange

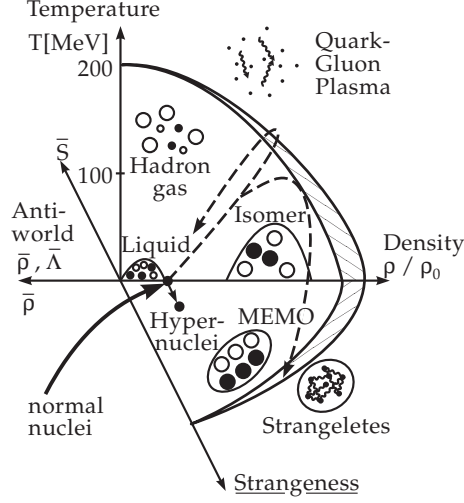


Figure 1: Sketch of the nuclear matter phase diagram with its extensions to strangeness and to the antiworld.

quarks is nearly equal to the number of massless up or down quarks and saturated SQM is nearly charge neutral. This simple picture does not hold for small baryon numbers. Finite size effects shift unavoidably the mass of strangelets to the metastable regime. Moreover strangelets can have very high charge to mass ratios for low baryon numbers. This behaviour is well known from normal nuclei. Therefore, instead of long-lived nearly neutral objects, strangelet searches in heavy ion experiments have to cope with short-lived highly charged objects [2] !

On the other hand, metastable exotic multihypernuclear objects (MEMOs) consisting of nucleons and hyperons have been proposed [3] which extend the periodic system of elements into a new dimension. MEMOs have remarkably different properties as compared with known nuclear matter as e.g. being negatively charged while carrying a positive baryon number! Even purely hyperonic matter has been predicted [4]. These rare composites would have a very short lifetime, at the order of the lifetime of the Λ . Central relativistic heavy ion collisions provide a prolific source of hyperons and hence, possibly, the way for producing MEMOs. Again, heavy ion experiments looking for these exotic composites have to deal with very short-lived highly charged objects!

2 Hyperon-rich Matter in Neutron Stars

Strangeness, in form of hyperons, appears in neutron star matter at a moderate density of about 2 – 3 times normal nuclear matter density $\rho_0 = 0.15 \text{ fm}^{-3}$ as shown by Glendenning within the Relativistic Mean Field (RMF) model [5]. These new species have considerable influences on the equation of state and the global properties of neutron stars.

On the other side, much attention has been paid in recent years to the possible onset of kaon condensation as the other hadronic form of strangeness in neutron stars. Most recent calculations based on chiral perturbation theory [6] show that kaon condensation may set in at densities of $(3 - 4)\rho_0$. Nevertheless, these calculations do not take into account the presence of hyperons which may already occupy a large fraction of matter when the kaons possibly start to condense [7].

Below I present new results from our recent paper [8], where the properties of neutron matter with hyperons were studied in detail. We use the extended version of the relativistic mean field (RMF) model and constrain our parameters to the available hypernuclear data and to the kaon nucleon scattering lengths.

2.1 The Model with Hyperons

The implementation of hyperons within the RMF approach is straightforward. SU(6)-symmetry is used for the vector coupling constants and the scalar coupling constants are fixed to the potential depth of the corresponding hyperon in normal nuclear matter [4]. We choose

$$U_{\Lambda}^{(N)} = U_{\Sigma}^{(N)} = -30 \text{ MeV} \quad , \quad U_{\Xi}^{(N)} = -28 \text{ MeV} \quad . \quad (1)$$

Note that a recent analysis [9] comes to the conclusion that the potential changes sign in the nuclear interior, i.e. being repulsive instead of attractive. In this case, Σ hyperons will not appear at all in our calculations.

The observed strongly attractive $\Lambda\Lambda$ interaction is introduced by two additional meson fields, the scalar meson $f_0(975)$ and the vector meson $\phi(1020)$. The vector coupling constants to the ϕ -field are given by SU(6)-symmetry and the scalar coupling constants to the σ^* -field are fixed by

$$U_{\Xi}^{(\Xi)} \approx U_{\Lambda}^{(\Xi)} \approx 2U_{\Xi}^{(\Lambda)} \approx 2U_{\Lambda}^{(\Lambda)} \approx -40 \text{ MeV} \quad . \quad (2)$$

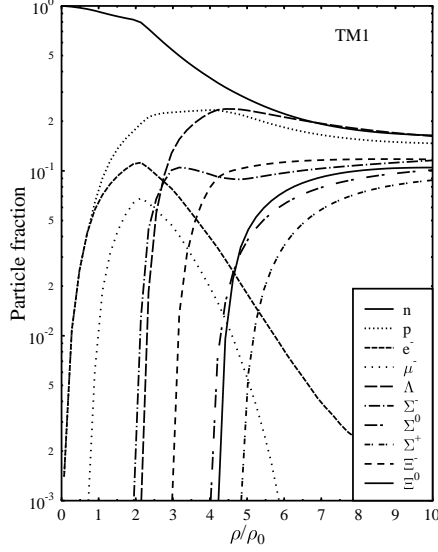


Figure 2: The composition of neutron star matter with hyperons which appear abundantly in the dense interior.

Note that the nucleons are not coupled to these new fields.

2.2 Neutron Stars with Hyperons

Fig. 2 shows the composition of neutron star matter for the parameter set TM1 with hyperons including the hyperon-hyperon interactions.

Up to the maximum density considered here all effective masses remain positive and no instability occurs. The proton fraction has a plateau at $(2 - 4)\rho_0$ and exceeds 11% which allows for the direct URCA process and a rapid cooling of a neutron star. Hyperons, first Λ 's and Σ^- 's, appear at $2\rho_0$, then Ξ^- 's are populated already at $3\rho_0$. The number of electrons and muons has a maximum here and decreases at higher densities, i.e. the electro-chemical potential decreases at high densities. The fractions of all baryons show a tendency towards saturation, they asymptotically reach similar values corresponding to spin-isospin and hypercharge-saturated matter. Hence, a neutron star is more likely a giant hypernucleus!

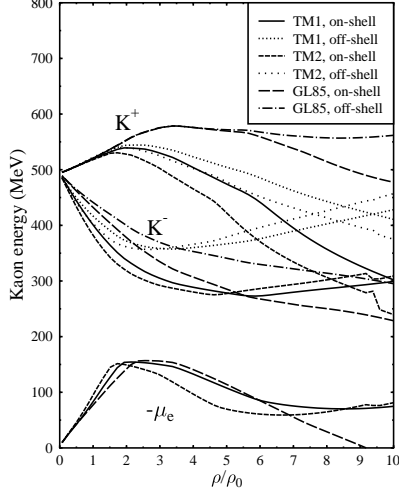


Figure 3: The effective energy of the kaon and the antikaon. and the electrochemical potential. Kaon condensation does not occur over the whole density region considered.

2.3 Kaon Condensation ?

In the following we adopt the meson-exchange picture for the KN-interaction simply because we use it also for parametrizing the baryon interactions. We start from the following Lagrangian

$$\mathcal{L}'_K = D_\mu^* \bar{K} D^\mu K - m_K^2 \bar{K} K - g_{\sigma K} m_K \bar{K} K \sigma - g_{\sigma^* K} m_K \bar{K} K \sigma^* \quad (3)$$

with the covariant derivative

$$D_\mu = \partial_\mu + ig_{\omega K} V_\mu + ig_{\rho K} \vec{\tau} \vec{R}_\mu + ig_{\phi K} \phi_\mu \quad . \quad (4)$$

The coupling constants to the vector mesons are chosen from SU(3)-relations. The scalar coupling constants are fixed by the s-wave KN-scattering lengths. We have found that this leads to an \bar{K} -optical potential around $U_{\text{opt}}^{\bar{K}} = -(130 \div 150)$ MeV at normal nuclear density for the various parameter sets used. This is between the two families of solutions found for Kaonic atoms [10]. The onset of s-wave kaon condensation is now determined by the condition $-\mu_e = \mu_{K^-} \equiv \omega_{K^-}(k=0)$.

The density dependence of the K and \bar{K} effective energies is displayed in Fig. 3. The energy of the kaon is first increasing in accordance with

the low density theorem. The energy of the antikaon is decreasing steadily at low densities. With the appearance of hyperons the situation changes dramatically. The potential induced by the ϕ -field cancels the contribution coming from the ω -meson. Hence, at a certain density the energies of the kaons and antikaons become equal to the kaon (antikaon) effective mass, i.e. the curves for kaons and antikaons are crossing at a sufficiently high density. At higher densities the energy of the kaon gets even lower than that of the antikaon! Since the electrochemical potential never reaches values above 160 MeV here antikaon condensation does not occur at all. We have checked the possibility of antikaon condensation for all parameter sets and found that at least 100 MeV are missing for the onset of kaon condensation in contrast to previous calculations disregarding hyperons [6].

3 Strange Antiworld

There are evidences for strong scalar and vector potentials in nuclear matter. Already in 1956 Dürre and Teller proposed a relativistic model with strong scalar and vector potentials to explain the saturation of nuclear forces [11] and found a scalar potential of $U_s = am_N\phi$ where ϕ is a scalar field and a is a coupling constant. This was the first version of the RMF model discussed above, where $U_s = g_\sigma\sigma$, and its extension, the Relativistic Brückner-Hartree-Fock (RBHF) [12] calculations, where the scalar potential is the scalar part of the self-energy of the nucleon $U_s = \Sigma_s(p_N)$. In the chiral $\sigma\omega$ model [13] one finds $U_s = m_N\sigma/f_\pi - m_N$ which incorporates the (approximate) chiral symmetry at the underlying QCD Lagrangian. Here f_π is the pion decay constant. Besides these models based on a hadronic description there exists effective models dealing with constituent quarks, like the Nambu–Jona-Lasinio (NJL) model and models based on QCD sum rules [14]. These models can be linked to hadronic observables in the dense medium by using the low density expansion of the quark condensate which gives $U_s = -\frac{m_N\sigma_N}{m_\pi^2 f_\pi^2}\rho_N$, where $\sigma_N \approx 45$ MeV is the pion-nucleon sigma term.

Astonishingly, *all* these approaches come to the same conclusion, namely that the scalar potential is as big as

$$U_s = -(350 \div 400) \text{ MeV } \rho_N/\rho_0 \quad (5)$$

for moderate densities! This strong scalar attraction has to be compensated

by a strong repulsion to get the total potential depth of nucleons correct. Hence, one finds for the vector potential

$$U_v = (300 \div 350) \text{ MeV } \rho_N/\rho_0 \quad . \quad (6)$$

These big potentials are in fact needed to get a correct spin-orbit potential. The idea of Dürre and Teller [11] was that the antinucleons feel the difference of these two potentials, i.e.

$$U_{\bar{N}} = U_s - U_v = -(650 \div 750) \text{ MeV } \rho_N/\rho_0 \quad (7)$$

which is already comparable to the mass of the nucleon. Note that the extrapolation to high densities is quite dangerous as effects nonlinear in density might get important. It is already known from RMF models that the scalar potential saturates at high densities instead of growing steadily. RBHF calculations show that this might be also true for the vector potential. With this in mind one can extrapolate to higher densities and finds that the field potentials get overcritical at $\rho_c = (3 - 7)\rho_0$ which was first pointed out by Mishustin [15]. At this critical density the potential felt by the antinucleons is equal to $U_{\bar{N}} = 2m_N$, the negative energy states are diving in the positive continuum and this allows for the spontaneous nucleon-antinucleon pair production. This has certain parallels to the spontaneous e^+e^- production proposed by Pieper and Greiner [16]. Assuming SU(6)-symmetry one gets for Λ 's

$$U_v^\Lambda = (200 \div 230) \text{ MeV } \rho_N/\rho_0 \quad (8)$$

and combining with hypernuclear data this gives then for the total $\bar{\Lambda}$ potential

$$U_{\bar{\Lambda}} = U_s^\Lambda - U_v^\Lambda = U_\Lambda - 2U_v^\Lambda = -(430 \div 500) \text{ MeV } \rho_N/\rho_0 \quad . \quad (9)$$

In the hyperon-rich medium additional fields will enhance this potential. Assuming again SU(6)-symmetry one can estimate the vector potential coming from the ϕ meson

$$V_v^\Lambda = \frac{2m_\omega^2}{9m_\phi^2} U_v \cdot f_s \approx 40 \text{ MeV } \rho_B/\rho_0 \cdot f_s \quad (10)$$

where f_s is the total strangeness fraction. The corresponding strange scalar potential is in principle unknown but definitely higher than the strange vector

potential to explain the strongly attractive $\Lambda\Lambda$ interaction seen in double Λ hypernuclei. Hence one gets at least an additional $\bar{\Lambda}$ potential of

$$V_{\bar{\Lambda}} = V_s^{\Lambda} - V_v^{\Lambda} \approx -120 \text{ MeV } \rho_B/\rho_0 \cdot f_s \quad (11)$$

in the hyperon-rich medium.

These strong antibaryon potentials will have certain impacts for heavy ion reactions. Proposed signals for antiprotons are: enhanced subthreshold production [15], change of the slope of the excitation function [15], apparent higher temperatures [17], which have indeed been measured at GSI [18]. Nevertheless, a recent analysis indicates that the antiproton potential might be quite shallow at normal nuclear density, around $U_{\bar{p}} = -100 \text{ MeV}$ [19]. Possible other signals include: enhanced antihyperon production [15], strong antiflow of antibaryons [20], cold baryons from tunnelling [15], cold kaons from annihilation in the medium (the phase space of the reaction $\bar{\Lambda} + p \rightarrow K^+ + \pi's$ is reduced by $U_{\bar{\Lambda}} + U_N - U_K \approx -600 \text{ MeV } \rho_N/\rho_0$ compared to the vacuum), enhanced pion production due to the abundant annihilation processes which would also enhance the entropy. Definitely, more elaborate work is needed to pin down the possible signals from the critical phenomenon of the antiworld.

We conclude this section with a brief comment concerning the limitations of the RMF model. This is clearly an effective model which successfully describes nuclear phenomenology in the vicinity of the ground state. On the other hand, this model does not respect chiral symmetry and the quark structure of baryons and mesons. Also negative energy states of baryons and quantum fluctuations of meson fields are disregarded. These deficiencies may affect significantly the extrapolations to high temperatures, densities or strangeness contents.

Acknowledgements

This paper is dedicated to Prof. Walter Greiner on the occasion of his 60th birthday. I am indebted to him for guiding me to the fascinating field of hypermatter and antimatter and his continuous support. I thank my friends and colleagues A. Diener, C.B. Dover, A. Gal, Carsten Greiner, and especially I.N. Mishustin and H. Stöcker for their help and collaboration which made this work possible.

References

- [1] C. Greiner and J. Schaffner, in *Quark-Gluon Plasma 2*, Ed. R.C. Hwa (World Scientific, Singapore, 1995), p. 635
- [2] C. Greiner, A. Diener, J. Schaffner, H. Stöcker, Nucl. Phys. **A566**, 157 (1994)
- [3] J. Schaffner, C. Greiner, H. Stöcker, Phys. Rev. **C46**, 322 (1992)
- [4] J. Schaffner, C.B. Dover, A. Gal, C. Greiner, H. Stöcker, Phys. Rev. Lett. **71**, 1328 (1993) and Ann. of Phys. (N.Y.) **235**, 35 (1994)
- [5] N.K. Glendenning, Astrophys. J. **293**, 470 (1985)
- [6] G.E. Brown, C.-H. Lee, M. Rho, V. Thorsson, Nucl. Phys. **A567**, 937 (1994)
- [7] J. Schaffner, A. Gal, I.N. Mishustin, H. Stöcker, W. Greiner, Phys. Lett. **B334**, 268 (1994)
- [8] J. Schaffner and I.N. Mishustin, Phys. Rev. **C53**, 1416 (1996)
- [9] J. Mares, E. Friedman, A. Gal, B.K. Jennings, Nucl. Phys. **A594**, 311 (1995)
- [10] E. Friedman, A. Gal, C.J. Batty, Phys. Lett. **B308**, 6 (1993); Nucl. Phys. **A579**, 518 (1994)
- [11] H.P. Dürr and E. Teller, Phys. Rev. **101**, 494 (1956)
- [12] L.S. Celenza, A. Pantziris, C.M. Shakin, W.D. Sun, Phys. Rev. **C45**, 2015 (1992)
- [13] J. Boguta, Phys. Lett. **120B** 34 (1983)
- [14] T.D. Cohen, R.J. Furnstahl, D.K. Griegel, Phys. Rev. Lett. **67**, 961 (1991)

- [15] I.N. Mishustin, Yad. Fiz. (Sov. J. Nucl. Phys.) **52**, 1135 (1990), J. Schaffner, I.N. Mishustin, L.M. Satarov, H. Stöcker, W. Greiner, Z. Phys. **A341**, 47 (1991), I.N. Mishustin, L.M. Satarov, J. Schaffner, H. Stöcker, W. Greiner, J. Phys. **G19**, 1303 (1993)
- [16] W. Pieper and W. Greiner, Z. Phys. **A218** 327 (1969)
- [17] V. Koch, G.E. Brown, C.M. Ko, Phys. Lett. **B265**, 29 (1991)
- [18] A. Schröter, E. Berdermann, H. Geissel, P. Kienle, W. König, A. Gillitzer, J. Homolka, F. Schumacher, H. Ströher, B. Povh, Nucl. Phys. **A553** (1993) 775c
- [19] St. Teis, W. Cassing, T. Maruyama, U. Mosel, Phys. Rev. **C50**, 388 (1994)
- [20] A. Jahns, C. Spieles, H. Sorge, H. Stöcker, W. Greiner, Phys. Rev. Lett. **72**, 3464 (1994)